

LEGIBILITY NOTICE

A major purpose of the Technical Information Center is to provide the broadest dissemination possible of information contained in DOE's Research and Development Reports to business, industry, the academic community, and federal, state and local governments.

Although a small portion of this report is not reproducible, it is being made available to expedite the availability of information on the research discussed herein.

LA-UR--88-599

DE88 006456

TITLE REMOTE TEMPERATURE MEASUREMENT INSTRUMENTATION FOR A
HEATED ROTATING TURBINE DISK

AUTHOR(S) S. S. Lutz, W. D. Turley, EG&G
H. M. Borella (Consultant, B. W. Noel, MEE-5
M. R. Cates, Engineering Technology Application Center
M. R. Probert, Delco Electronics Corp.

SUBMITTED TO

DISCLAIMER

This report was prepared as an account of work sponsored by an agency of the United States Government. Neither the United States Government nor any agency thereof, nor any of their employees, makes any warranty, express or implied, or assumes any legal liability or responsibility for the accuracy, completeness, or usefulness of any information, apparatus, product, or process disclosed, or represents that its use would not infringe privately owned rights. Reference herein to any specific commercial product, process, or service by trade name, trademark, manufacturer, or otherwise does not necessarily constitute or imply its endorsement, recommendation, or favoring by the United States Government or any agency thereof. The views and opinions of authors expressed herein do not necessarily state or reflect those of the United States Government or any agency thereof.

By acceptance of this article the publisher recognizes that the U.S. Government retains a nonexclusive, royalty-free license to publish or reproduce the published form of this contribution or to allow others to do so, for U.S. Government purposes.

The Los Alamos National Laboratory requests that the publisher identify this article as work performed under the auspices of the U.S. Department of Energy.

MASTER

Los Alamos

Los Alamos National Laboratory
Los Alamos, New Mexico 87545

DISTRIBUTION OF THIS DOCUMENT IS UNLIMITED

REMOTE TEMPERATURE-MEASUREMENT INSTRUMENTATION FOR A HEATED ROTATING TURBINE DISK

S. S. Lutz
Scientific Specialist II
and
W. D. Turley
Senior Scientist
EG&G Energy Measurements, Inc.
130 Robin Hill Road
Goleta, CA 93116

H. M. Borella
Consultant
and
B. W. Noel
Group Leader
Los Alamos National Laboratory
P. O. Box 1663
Los Alamos, NM 87545

M. R. Cates
Development Staff Member
Engineering Technology Applications Center
P. O. Box P
Oak Ridge, TN 37831

M. R. Probert
Software Engineer
Delco Electronics Corporation
6767 Hollister Ave.
Goleta, CA 93116

ABSTRACT.

Thermographic-phosphor (TP) remote temperature sensors were installed on a turbine disk and subjected to thermal and centrifugal stresses in a spin-pit test. The sensors were placed at three different radii on the disk, which was run at 6600, 9330, 11400, and 13200 rpm at nominal temperatures of ambient, 300°F, 600°F, 900°F, and 1250°F (149°C, 316°C, 482°C, and 677°C, respectively).

The paper gives details of the TP temperature-measurement method, phosphor bonding to the disk, calibration, optical-system design, and electronics instrumentation.

The temperatures measured by the TP sensors were compared with those measured by thermocouples mounted on the disk. A number of the thermocouples behaved erratically after we operated the disk at 677°C for an extended period. Nevertheless, for those cases where they could be compared with confidence, the agreement between the TP sensors and the thermocouples was good.

INTRODUCTION.

This paper describes the successful application of thermographic-phosphor (TP) technology to surface-temperature measurements on a rapidly spinning turbine disk. This experiment was part of a program whose goal is measuring surface temperatures on first-stage rotor blades and stator vanes in an operating turbine engine.¹

Thermographic phosphors are materials whose optical-emission properties exhibit a unique functional dependence on their temperature. The phosphor temperature sensitivity is believed to result from thermally activated nonradiative quenching, accompanied by population redistribution between competing emitting states.² The temperature dependence of the phosphor emission is manifested both in the characteristic decay time and the intensities of peaks in the emission spectrum. After appropriate excitation by ultraviolet or higher energy, either the ratio of two emission-line intensities or the decay time of some selected line can be used to determine temperature.

Our instrumentation efforts have centered on measuring phosphor decay times as a function of temperature. Although spectral analysis of the phosphor emission will also yield temperature information,³ our limited investigation into this technique suggests that it is less precise and more susceptible to systematic error than decay-time measurements when used on periodically moving systems.

The use of thermally dependent phosphor luminescence as a sensor enables one to make temperature measurements in remote or hostile environments. Further, the use of fast pulse techniques enables one to measure temperature on rapidly moving frames of reference with precise time resolution.⁴

The experiment reported here was carried out at a spin-pit facility at the United Technologies Research Center (UTRC) in Hartford, Connecticut. The UTRC spin-pit measurements are commonly made at speeds of 1200, 6600, 9300, 11400, and 13200 rpm and at temperatures of 149°C, 316°C, 482°C, and 677°C. Our experiment plan was to instrument these four temperature points at the four faster speeds and at three different disk radii. This goal placed a number of new demands on our TP measurement system.

EXPERIMENT DETAILS.

A. Phosphor Selection and Characterization.

Several of the test points were located in temperature regions that have not previously been instrumented using this technique. Consequently, a substantial amount of time was spent finding TPs whose luminescence-decay times exhibit a functional dependence on temperature in 100°F(56°C)-wide regions bracketing each of the chosen test temperatures. Assuming a simple functional dependence of decay time on temperature was not a sufficient criterion for this experiment. The value of the decay constant must be short enough that the phosphor intensity will change a significant amount in the available measurement-time aperture. This time aperture was $\approx 200\mu\text{s}$ at 13200 rpm. The aperture is limited by the fact that we could view only a small portion of the rotating disk with our optics. The region of uniform optical collection was limited to approximately 20° of arc. Working with materials that exhibit decay times less than the 200- μs aperture insures the measurement of at least one full phosphorescent decay time at the highest rotational speeds. Longer decay times can be measured, but with some loss in accuracy.

Some TPs (including many oxysulfides) that are useful for measuring relatively low temperatures tend to degrade at higher temperatures. For this experiment, all the TPs must be able to be cycled to the highest temperature, 677°C, without change in the decay time or significant loss of emission intensity. In a simple screening test, each candidate TP was kept at 677°C for 24 hours. The temperature was then lowered to a level at which the calibration and sensitivity of the phosphor could be checked. This procedure was repeated for three or four days. The phosphors subjected to this test were bound to IN-100 inconel-alloy plates using a binder of choice. Several TP candidates, as well as a number of possible binders, were rejected on the basis of this test. Table I lists the phosphors used for this experiment, along with their active temperature range and the wavelength of the emission maximum. To cover the four temperatures required three TPs. $\text{La}_2\text{O}_3\text{:Eu}$ (europium-doped lanthanum oxysulfide) was used to measure the 149°C point, $\text{YVO}_4\text{:Dy}$ (dysprosium-doped yttrium vanadate) the 316°C point, and $\text{Mg}_2(\text{F})\text{GeO}_4\text{:Mn}$ (manganese-doped magnesium fluorogermanate) the 482°C and 677°C points.

B. UTRC Spin-Pit Configuration.

The basic experiment layout is shown in Figure 1. The spin pit is configured such that the instrumented disk rotates horizontally in a vacuum chamber. The disk is heated with an inductive rf heater. The lid contains two optical ports. A 13-cm-diam port is located directly over and parallel to the disk. The vertical distance from the port to the disk is 58 cm. A 5-cm-diam port is located over the axis of rotation and is angled such that the window is normal to the direction of view. Both ports have a clear optical path to a common area of the disk. The 5-cm port was used to pass excitation light, and the 13-cm port was used to collect the TP emission.

A pulsed nitrogen laser with an ultraviolet optical-output wavelength of 337 nm was used to excite the phosphors. Because the laser beam has considerable divergence (3 by 7 mrad), focusing optics were used to create a spot of ≈ 1 -cm-diam on the disk. A gimbal-mounted mirror was used to select which of the three phosphor radii was irradiated.

The uniformity of collection as a function of position in the object plane was a primary concern in the design of the collection optics. Any spatial shading, due either to the optical collection or photomultiplier-tube (PMT) photocathode nonuniformity, will distort the decay-time data, possibly causing systematic error in the temperature measurement.

Figure 2 is a series of ray traces showing how the collection optics image the TP emission onto the PMT photocathode. A 200-mm-focal-length, 100-mm-diam collection lens was used to focus the phosphor emission onto a 25-mm-square field stop with a reduction of approximately 2:1. A 90-mm-focal-length, 60-mm-diam field lens was used to provide a nearly uniform illumination of the photocathode. Figures 2a and 2b show the results of a bundle of rays launched on-axis and 2 cm off-axis. As shown in the detector-plane spot diagrams in Figure 2, the ray pattern impinging on the detector is changed minimally.

A narrow-band interference filter, centered around the appropriate emission line, and a Schott glass long-pass filter were placed in the plane of the field stop. The Schott filter was necessary to provide a sufficient amount of rejection of the excitation light.

Figure 3 is a photograph of the instrumentation disk. The instrumentation supplied by UTRC consists of thermocouples, welded directly to the disk, and thin-film strain gauges with thermocouples welded onto the gauge foil. The locations of the thermocouples that we used for data analysis are also shown in Figure 3. The electrical leads for the UTRC instrumentation are connected to slip rings and from there to a computerised read-out package.

The nine spots on the left side of the disk in Figure 3 are our three TPs that cover the required temperature ranges. Each was applied at three radii to mimic the standard UTRC instrumentation positions, hence the array of nine TP spots.

Measurement timing originated with a "once-around" trigger provided by an inductive pick-off from the rotor. This signal was first counted down by a factor of 20 to 25. This digital count-down circuitry was used to reduce the ≈ 200 -Hz frequency of the rotor disk to less than the 10-Hz maximum repetition rate of our nitrogen laser.

The trigger was then delayed with a high-precision low-jitter time-delay unit so that the laser light arrived at the disk coincident with the desired phosphor spot. By varying the amount of delay, we could select the appropriate phosphor for the temperature range being measured. Because the laser is spark-gap-initiated, it has an inherent 200-500 ns of jitter between the trigger time and the fire time. To overcome this, we used a silicon detector, viewing the reflection off one of the laser lenses, to trigger the digitiser.

The digitiser is a LeCroy model TR8828b/mm8103A contained in a CAMAC crate. The crate is controlled by an LSI-11 micro-computer. Data were stored on a Winchester hard disk. An in-house-designed software package was used to drive the instrumentation and analyse the data. Typically, 100 pulses were averaged to enhance the signal-to-noise ratio.

CALIBRATION.

Prior to the experiment, the TPs were applied to the disk and calibration data (decay time vs temperature) were collected at our own laboratories. A large oven was built for the calibration. An NBS-traceable thermocouple⁸ was attached to the disk in the region of the test phosphors. The calibration procedure was to heat the disk to $\approx 700^\circ\text{C}$, then slowly cool the oven at a rate of $\approx 1^\circ\text{F}/\text{min}$ ($0.6^\circ\text{C}/\text{min}$). We took data every 5°F (3°C) as the oven cooled, bracketing the measurement points by nearly 50°F (28°C). These calibration data are shown in Figure 4.

The solid line in Figure 4 is the result of a least-squares exponential fit to the data:

$$T = Ae^{br},$$

where T is the thermocouple temperature, r is the measured decay time, and A and b are the fitting parameters. This expression was used as the calibration function in exponential regions of the calibration curve. In nonexponential regions, a calibration point was calculated using a linear interpolation between the two adjacent points. Measurement-precision values were obtained from the calibration data by calculating a sigma value, using the exponential fit as the expected value, from

$$\sigma = \sqrt{\frac{1}{n-1} \sum_{i=1}^n \left(t(i) - \frac{\ln T - \ln A}{b} \right)^2},$$

where n is the number of elements in the set. A two-sigma error value based on this calculation is shown in Figure 4. These numbers give the precision of the calibration.

DATA ANALYSIS.

Figure 5 shows a typical TP decay curve. Decay times were calculated by doing a linear regression to the natural logarithm of the data. This calculation is made over a limited region of the emission curve. The dotted line in Figure 5 marks the end of a "dead" time, which is employed to avoid laser-excitation artifacts in the data. The origin of the spike lies both in scattered laser light and prompt disk-contaminant fluorescence. After the dead time, a window of predetermined width is used to select the part of the emission curve to be analysed. The window boundaries are shown in Figure 5 as the two solid lines crossing the data at ≈ 35 and $75 \mu\text{s}$. This window starts at 90% of the pulse height present after the dead time and ends at 30%. Decay times are calculated using the data contained within this window.

Figure 6a is a semilog plot of the data contained within the window shown in Figure 5. Also shown in this figure is a plot of the calculated curve using the decay time extracted by the least-squares algorithm. Figures 6b, c, and d show similar data for the three other temperature ranges that were measured.

As previously stated, a known—and preferably uniform—collection efficiency over the measured region of the disk is necessary for accurate results. We verified the flatness of the optical field by measuring the phosphorescent decay of $\text{Mg}_2(\text{F})\text{GeO}_4:\text{Mn}$ at room temperature. The TP response was first measured while the disk was stationary. The decay time of this TP at room temperature is ≈ 3 ms. The stationary measurement was divided into measurements made at room temperature with the disk rotating. The results of this division are shown in Figure 7. The three pulses shown in this figure represent data taken at three different rotational speeds: 6600, 9300, and 11400 rpm.

Artifacts due to the laser-excitation pulse are clearly seen in the left side of Figure 7. At the higher rotational velocities, (Figure 7, curves b and c), the TP spot passes through the optical-collection region before the end of the $320\text{-}\mu\text{s}$ measurement time. This is the reason for the rolloff seen in curves b and c. Excluding the high-frequency noise, the excitation region, and the rolloff late in the pulse, these data show that the collection efficiency is uniform to within $\approx 5\%$.

There appears to be a slight tilt in the flat-field data. The trend is toward increasing sensitivity late in the field of view. An increase of approximately 5% is observed across the $320\text{-}\mu\text{s}$ window. The effect of the distortion on the decay time is nearly equal to the percentage change in the collection efficiency over the duration of one TP

decay time. The longest decay times that we measure are on the order of 100 μ s. At this level, the distortion will result in a 1.5% increase in the measured decay time over the actual decay time. Using the calibration curves in Figure 4, this translates to less than a $\pm 1.5^\circ\text{F}$ (0.8°C) correction in all cases.

Because the magnitude of this correction is small, we did not divide the data by the optical-field measurements. We were, however, careful to do our analysis in the flat region of the collection-efficiency curve.

RESULTS.

Table II shows a comparison of UTRC thermocouple-derived temperature data with the temperatures calculated from the TP decay-time data. The temperatures calculated from TP decay times and UTRC thermocouples all agree within 1% at both 6600 and 11400 rpm. The phosphor data were collected from the outer radial phosphor spot at 16.8 cm from the center of disk rotation. Thermocouple readings are taken from a variety of disk locations from thermocouples mounted directly to the disk surface (TC31, 15.5 cm from disk center) or on top of thin-film strain gauges (TC07 and TC08, 16.5 cm and 15.2 cm from the disk center, respectively).

The data collected at 6600 rpm were acquired during the early stages of the experiment, while the majority of disk thermocouples were operating reliably. Later in the experiment, when we required disk operation at an elevated temperature (677°C) for an extended period, a number of the disk thermocouples developed anomalous intermittent temperature readings. The breakdown in thermocouple output consistently resulted in a failure towards cooler temperature readings. This problem was possibly due to a combination of soft vinyl insulation over the thermocouple leads, an overheated disk bore, and centrifugal-force loading of the leads. These three factors could combine to create secondary junctions in the thermocouple leads, the symptom of which is an intermittent cold failure of the sensor.⁶ Thereafter, when thermocouple failure appeared, the thermocouple with the highest temperature reading was chosen as the most accurate and used to compare with the temperatures calculated from phosphor decay-time data.

The data taken at 6600 rpm (before the onset of thermocouple problems) established the relationship between the various UTRC disk-surface and strain-gauge-mounted thermocouples and the TP data. The strain-gauge-mounted thermocouples (TC07 and TC08) yield temperature values from 2% to 10% lower than the phosphors and the disk-surface-mounted thermocouples. These thermocouples are insulated from the disk surface by the thin-film strain gauges and are expected to be slightly cooler. At 11400 rpm, the disk-surface-mounted thermocouple (TC31) failed; however, a combination of good TC07 and TC08 data were obtained and are tabulated along with TP temperatures. There is good agreement ($\pm 3\%$) between the TP temperatures and TC07 and TC08 data.

To investigate the effect of disk rotational speed in more detail, a series of measurements was taken at 6600, 9300, and 11400 rpm at a single spot and at a fixed temperature. These data are tabulated in Table III. The phosphor data are taken from the outer radial spot 16.8 cm from the disk center) of $\text{Mg}_4(\text{F})\text{GeO}_6\text{:Mn}$ and are compared with disk-surface (TC31) and thin-film-strain-gauge-mounted (TC08) thermocouples. Again the agreement between thermocouple and TP temperatures is good.

In addition to measurements as a function of disk speed and temperature, TP decay-time measurements were made at three radial positions at fixed rpm (6600) and temperature ($\approx 315^\circ\text{C}$). The results of these experiments are given in Table IV. The thin-film-strain-gauge-mounted thermocouple TC08 gave good data throughout this experiment and is compared with the TP temperatures. The TP data show that temperature does not vary appreciably, after approximately 10 minutes of operation at speed, in the disk-web region between the 14.2-cm to 16.8-cm radial positions. However, the inner TP spot (radial position = 14.2 cm) was significantly lower in temperature than TC08 (radial position = 15.2 cm) when the experiment was initiated with a cool disk-bore temperature.

CONCLUSIONS.

We used TP to measure surface temperature on a rapidly spinning turbine disk at the UTRC spin-pit facility. Using the decay time of phosphor materials applied to the turbine disk, surface temperatures were measured at 149, 316, 482, and 677°C at disk rotational speeds of 6600 and 11400 rpm. Additional measurements were made at 677°C and 9300 rpm as well as at three radial positions (14.2, 15.5, and 16.8 cm from the center of disk rotation) at 6600 rpm and 316°C.

The temperatures measured with the TP technique agreed to within 4% of the nearest disk-thermocouple reading in all cases. The maximum difference between TP and thermocouple temperature readings exceeds the expected scatter based on the calibration-precision and thermocouple-accuracy measurements. However, at this point it is unclear whether the differences result from actual variations on the disk surface, the UTRC thermocouples, or the TP phosphor measurements.

ACKNOWLEDGMENTS.

The authors are pleased to acknowledge the support, cooperation, assistance, and helpful suggestions provided by many people, including Graham Fulton, Tony Dennis, and Bill Rioux from UTRC, Larry Franks from EG&G Energy Measurements, and Bill Stange from AFWAL/POTC. We especially wish to acknowledge the financial support provided by the Air Force Wright Aeronautical Laboratory.

REFERENCES.

1. Noel, B. W., *et al.* "Evaluating and Testing Thermographic Phosphors for Turbine-Engine Temperature Measurements," paper no. AIAA-87-1761, AIAA/SAE/ASME/ASME 23rd Joint Propulsion Conference, San Diego, CA (June, 1987).
2. Struck, C. W., and Fonger, W. H., "Quantum-Mechanical Treatment of Eu^{3+} $f \rightarrow 4f$ and $4f \rightarrow 4f$ Charge-Transfer-State Transitions in $\text{Y}_2\text{O}_3\text{S}$ and $\text{La}_2\text{O}_3\text{S}$," J. Chem. Physics 64, 1784 (1976).
3. Wickersheim, K. A., and Alves, R. V., "Recent Advances in Optical Temperature Measurement," Research & Development, p. 82. (December, 1979).
4. Cates, M. R., *et al.*, "Applications of Pulsed-Laser Techniques and Thermographic Phosphors to Dynamic Thermometry of Rotating Surfaces," Martin Marietta Energy Systems report no. K/TS-11,504 (1985).
5. Traceability to N.B.S. Tests nos. 80-00034 and 4393. Accuracy reported to within $\pm 1\%$ for standard thermocouple. The type-K thermocouple used for our calibration experiments matched within 1% when tested against the standard thermocouple at 149°C, 316°C, 482°C, and 649°C.
6. Graham Fulton, UTRC, private communication.

Table I

Phosphors used in this experiment, the range over which they work as thermometers, and the wavelength of the emission line that was used.

Phosphor Temperature Emission Range (°C) wavelength (nm)

$\text{La}_2\text{O}_3\text{S}:\text{Eu}^{3+}$ 100 - 260 537

$\text{YVO}_4:\text{Dy}^{3+}$ 290 - 450 574

$\text{Mg}_2(\text{F})\text{GeO}_6:\text{Mn}^{2+}$ 450 - 730 656

Table II

Summary of Temperature Data at 6600 and 11400 rpm Thermocouple (TC) versus Thermographic Phosphor (TP) Data

6600 rpm 11400 rpm

Measured Temperature (°C) Measured Temperature (°C)

TC07 TC08 TC31 TP TC07 TC08 TP (a) (b) (c) (d) (a) (b) (d) 148 143 153 159 147 - 152 301 302 317 323
329 - 341 461 468 489 491 502 - 517 - 643 664 656 - 648 645

a. Thermocouple mounted on top of thin-film strain gauge, 16.5 cm from disk center.

b. Thermocouple mounted on top of thin-film strain gauge, 15.2 cm from disk center.

c. Thermocouple mounted directly to disk-surface, 15.5 cm from disk center.

d. Phosphor radial position is 16.8 cm from disk center.

Table III

Measured Temperatures versus Disk Rotational Speed Thermocouple (TC) versus Thermographic Phosphor (TP) Data

Disk Speed (rpm) Temperature Measured (°C)

TC08 TC31 TP (a) (b) (c) 6600 640 666 647 9300 643 666 646 11400 648 668 645

a. Thermocouple mounted on top of thin-film strain gauge, 15.2 cm from disk center. b. Thermocouple mounted directly to disk surface, 15.5 cm from disk center. c. Phosphor radial position is 16.8 cm from disk center.

Table IV

Summary of Radial Temperature Measurements Thermocouple (TC) versus Thermographic Phosphor (TP) Data (Note a)

Phosphor Radial Position (cm) Measured Temperature (°C)

TC08 TP (b) 14.2 640 (630) 658 (602) 15.5 635 665 16.8 635 662

a. Disk rotational speed is held constant at 6600 rpm. b. Thermocouple mounted on top of thin-film strain gauge, 15.2 cm from disk center. c. Value in parenthesis refers to initial reading with a cool bore.

Figure Captions.

Figure 1. Schematic diagram of the experiment layout at the UTRC spin-pit facility.

Figure 2. Ray-trace and detector-plane spot diagrams of experiment collection optics.

Figure 3. Photograph of the instrumented turbine disk.

Figure 4. Calibration curves for the four temperature regions covered during the spin-pit experiment. Left to Right: $\text{La}_2\text{O}_2\text{S:Eu}$, $\text{YVO}_4\text{:Dy}$, and $\text{Mg}_4(\text{F})\text{GeO}_6\text{:Mn}$ (twice).

Figure 5. Reproduced typical TP luminescence-decay curve. The disk was rotating at 6600 rpm and the temperature was 307°F(153°C).

Figure 6a. Semilog plot of the data contained within the window region of Figure 5. The temperature is 153°C.

Figure 6b. Semilog plot of the data contained within the window region of Figure 5. The temperature is 326°C.

Figure 6c. Semilog plot of the data contained within the window region of Figure 5. The temperature is 489°C.

Figure 6d. Semilog plot of the data contained within the window region of Figure 5. The temperature is 677°C.

Figure 7. Flat-field data at three different speeds: 6600, 9300, and 11400 rpm.

Table I. Phosphors Used in This Experiment, the Range Over Which They Work as Thermometers, and the Wavelength of the Emission Line Used.

Phosphor	Temperature Range (°C)	Emission wavelength (nm)
LOS	100 - 260	537
YV	290 - 450	574
MFG	450 - 730	656

Table II. Summary of Temperature Data at 6600 and 11400 rpm. Thermocouple (TC) Versus Thermographic-Phosphor (TP) Data.

6600 rpm Measured Temperature (°C)				11400 rpm Measured Temperature (°C)		
TC07 ^a	TC08 ^b	TC31 ^c	TP ^d	TC07 ^a	TC08 ^b	TP ^d
148	143	153	159	147	---	152
301	302	317	323	329	---	341
461	468	489	491	502	---	517
---	643	664	656	---	648	645

^aThermocouple mounted on top of thin-film strain gauge, 16.5 cm from disk center.

^bThermocouple mounted on top of thin-film strain gauge, 15.2 cm from disk center.

^cThermocouple mounted directly to disk surface, 15.5 cm from disk center.

^dPhosphor radial position is 16.8 cm from disk center.

Table III. Measured Temperatures Versus Disk Rotational Speed. Thermocouple (TC) versus Thermographic-Phosphor (TP) Data.

Disk Speed (rpm)	Temperature Measured (°C)		
	TC08 ^a	TC31 ^b	TP ^c
6600	640	666	647
9300	643	666	646
11400	648	668	645

^aThermocouple mounted on top of thin-film strain gauge, 15.2 cm from disk center.

^bThermocouple mounted directly to disk surface, 15.5 cm from disk center.

^cPhosphor radial position is 16.8 cm from disk center.

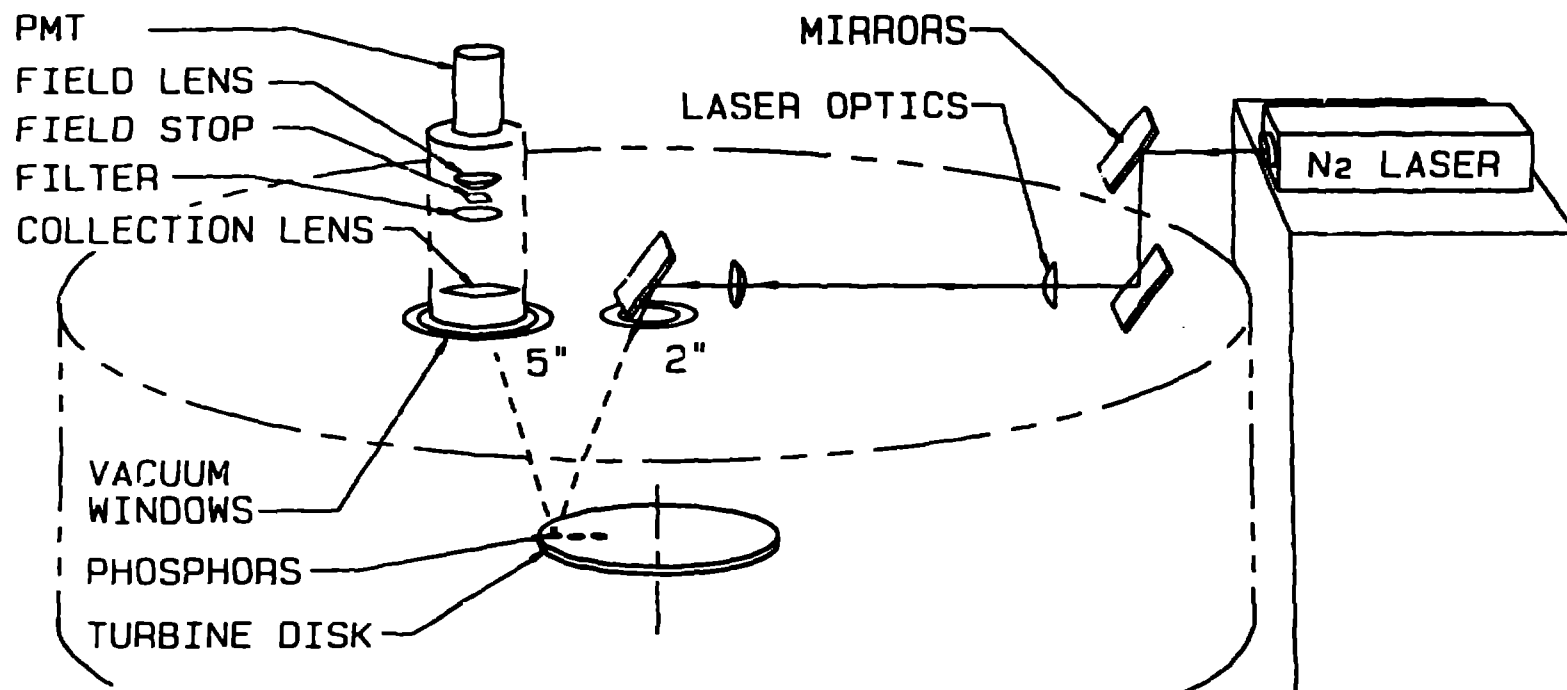
Table IV. Summary of Radial Temperature Measurements. Thermocouple (TC) versus Thermographic-Phosphor (TP) Data.^a

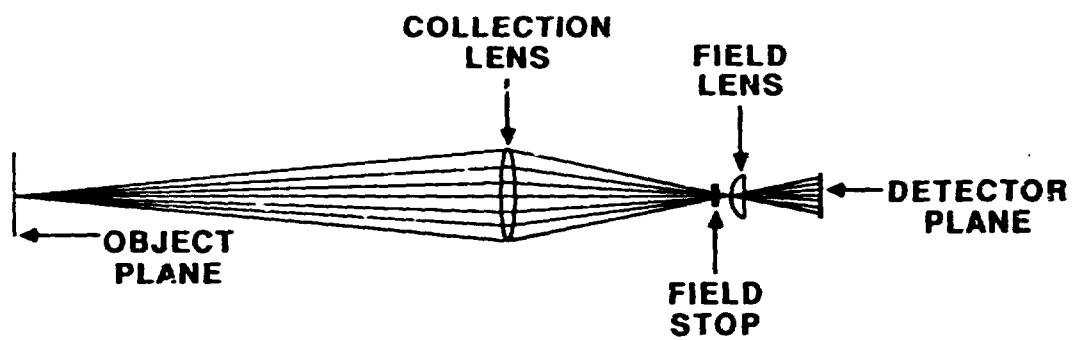
Phosphor Radial Position (cm)	Measured Temperature (°C)	
	TC08 ^b	TP
14.2	640 (630)	658 (602)
15.5	635	665
16.8	635	662

^aDisk rotational speed is held constant at 6600 rpm.

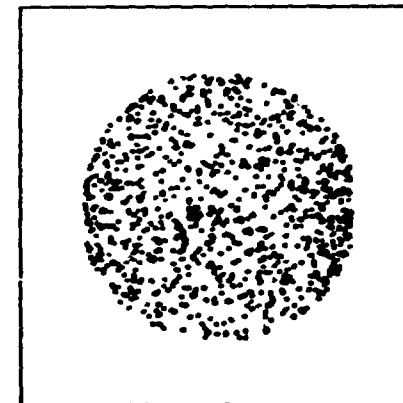
^bThermocouple mounted on top of thin-film strain gauge, 15.2 cm from disk center.

^cValue in parentheses refers to initial reading with a cool bore.





2a. OBJECT LOCATED ON AXIS



2b. OBJECT LOCATED 2.5 cm OFF AXIS

